

Crack propagation and residual stress in laminated Si₃N₄/BN composite structures

Zoran Krstic*, Vladimir D. Krstic

Mechanical and Materials Department, Queens' University, Kingston, ON, Canada K7L 3N6

Received 17 September 2010; received in revised form 2 March 2011; accepted 7 March 2011

Available online 14 April 2011

Abstract

The level of residual stress and crack propagation in a new generation of laminates, based on silicon nitride (Si₃N₄) layer and a mixture of boron nitride (BN) and alumina (Al₂O₃) interlayer, was presented. The structure consists of alternated concentric rings of Si₃N₄ separated by the weak BN interlayer possessing no planes of easy crack propagation and fracture resistance much larger than that of any classical planar laminates. The results on direction of crack propagation and residual stress in relation to inter-layer composition, the number of layers, and their thickness are investigated and reported. The effect of residual stress on crack propagation was studied by using Vickers indentation. The highest compressive residual stress of ~170 MPa was found in samples with five layers possessing an average layer thickness of ~310 × 10⁻⁶ m.

© 2011 Elsevier Ltd. All rights reserved.

Keywords: Composites; Residual stress; Crack propagation; Thermal expansion; Interfaces

1. Introduction

A new generation of laminated structures has been designed and fabricated using a modified slip casting method followed by pressureless sintering.^{1–3} Instead of layers being deposited in the planar form, as is the case with planar laminates, in the new design they are arranged in the form of concentric rings along the length of the structure thus avoiding the creation of plane for easy crack propagation.²

Two different laminate compositions (in the terms of inter-layer phase composition) were designed. The first one, consists of Si₃N₄ layers, and interlayers containing 10 wt.% of Si₃N₄ and 90 wt.% of BN marked as SN – (SN + BN); and the second one, consists of Si₃N₄ layers, and interlayers containing 50 wt.% of Al₂O₃ and 50 wt.% of BN marked as SN – (BN + Al₂O₃). In these types of structures the objective is to create interfacial layer sufficiently weak to allow crack deflection along the interface. On the other hand, the strength of the Si₃N₄ layer must be sufficiently high to prevent an easy crack initiation at the surface of the next layer. The residual stress is known to strongly affect mechanical behaviour of the laminated composite by controlling

the crack propagation at the interface between the two dissimilar materials.^{4,5} According to He et al., there are three possibilities for the crack propagation: the crack may arrest at the interface under compressive stress, it may penetrate the interface, or it may deflect from the interface. The structural model which will provide this to take place is proposed in Fig. 1.

During the fabrication of composites with two dissimilar materials (Si₃N₄ layers and BN – Al₂O₃ interlayer) residual stresses will arise due to the mismatch in thermal expansion and differences in elastic properties.^{6–8} In the case of laminates with different ceramics, the differences in shrinkage during sintering will also contribute to the residual stress.⁹ Perhaps, the most important factor which contributes to the rise in residual stress is the difference in the linear coefficient of thermal expansion between the two materials used to fabricate laminates. The residual strain, responsible for the creation of residual stress, which develops in a composite laminate consisting of materials with different thermal expansion coefficients, as proposed by the Oechsner et al.¹⁰ can be expressed by equation:

$$\varepsilon_M = \int_T^{T_0} (\alpha_2 - \alpha_1) dT \quad (1)$$

where α_1 and α_2 are the thermal expansion coefficients of the two materials and dT is the temperature difference $T_1 - T_0$.

* Corresponding author. Fax: +1 6135336610.
E-mail address: krsticz@queensu.ca (Z. Krstic).

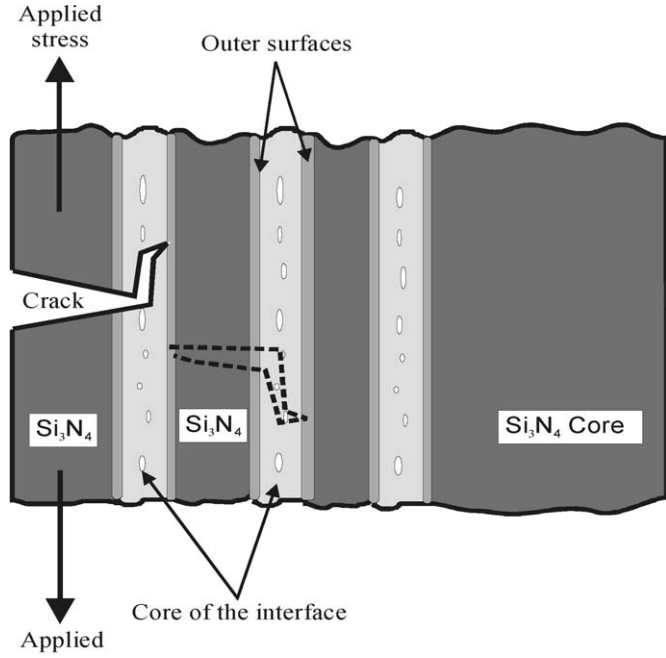


Fig. 1. One half of the structural model; the interfacial layer with porous and weak core and a high density strong outer surface well bonded to Si_3N_4 layer.

In the Si_3N_4 laminates the residual bi-axial compressive stress in the Si_3N_4 is given by Blugan et al.¹¹:

$$\sigma_C = -\frac{\varepsilon_M \cdot E'_1}{1 + (t_1 \cdot E'_1 / t_2 \cdot E'_2)} \quad (2)$$

where $E' = E/(1 - \nu)$, E_1 and E_2 are Young's modulus of materials with thermal expansion coefficients of α_1 and α_2 , respectively, ν is the Poisson's ratio and t_1 and t_2 are the thickness of the layer 1 and layer 2, respectively. In the interlayer ($\text{Al}_2\text{O}_3 + \text{BN}$) which has larger thermal expansion coefficient compared to silicon nitride, the bi-axial tensile stress is given by¹¹:

$$\sigma_T = -\sigma_C \frac{t_1}{t_2} \quad (3)$$

If t_1/t_2 approaches 0 then the bi-axial stress in material with lower thermal expansion coefficient (i.e. Si_3N_4) reduces to:

$$\sigma_C = -\frac{\varepsilon_M \cdot E_1}{1 - \nu} \quad (4)$$

and the stress in the material with larger thermal expansion coefficient vanishes (σ_T approaches 0).

The effect of residual stress on crack propagation was studied using Vickers indentation by Hsueh and Evans⁶ who developed a method of measuring the residual stress in a ceramic matrix by comparing the growth of crack from indentations made in unstressed and stressed materials. The same method was used by Marshal and Lawn¹² to evaluate the residual stress in tempered glass. In 1994 Zeng and Rowcliffe¹³ developed a method of mapping the residual stress in glass. First, they introduced a residual stress in the glass by applying high external loads. Then, using low loads, small indentations were made at various angles and distances from the cracks extending from the large

indentations. It was then possible to map the residual stress field created on the materials surface by the indentation.

By using indentation fracture mechanics theory it has been possible to determine the fracture toughness, K_{IC} , of the material by measuring the load and crack length C_0 , via equation of the form¹⁴:

$$K_{IC} = \alpha \cdot \left(\frac{E}{H}\right)^{1/2} \cdot \left(\frac{P}{C_0^{3/2}}\right) \quad (5)$$

where P is the indentation loads, α is an empirical geometric constant, and E and H are Young's modulus and hardness, respectively. Following Zeng and Rowcliffe¹³ it has been shown that, under the influence of a prevailing residual stress, σ_a , the crack will assume a new equilibrium length, C , when the surface of the specimen is loaded at the same indentation load, P , as in the unstressed case. At equilibrium, the crack will then experience composite stress intensity, described by the fracture toughness, K_{IC} , and is given by the expression:

$$K_{IC} = \alpha \cdot \left(\frac{E}{H}\right)^{1/2} \cdot \left(\frac{P}{C_0^{3/2}}\right) \pm \psi \sigma_a C^{1/2} \quad (6)$$

The first term in Eq. (6) represents the stress intensity due to the indentation load, P , and the second term corresponds to the contribution of a prevailing residual stress. The sign \pm refers to the tensile or compressive stress. Under the tensile stress, the second term is added to the first term, and under the compressive stress the second term is subtracted from the first term. In Eq. (6), ψ is a crack geometry factor and describes the nature of the surface-to-depth ratio of the crack dimensions. The commonly used value for ψ for Vickers indenter is $\sqrt{\pi}$ (Lawn).¹⁵ Combining Eqs. (5) and (6) and noting that the same peak load is involved in both expressions, the unknown residual stress is obtained through the expressions:

$$\sigma_T = K_{IC} \cdot \left[\frac{1 - (C_0/C)^{3/2}}{\psi \cdot \sqrt{C}} \right] \quad (7)$$

$$\sigma_C = -K_{IC} \cdot \left[\frac{1 - (C_0/C)^{3/2}}{\psi \cdot \sqrt{C}} \right] \quad (8)$$

where σ_T and σ_C represent residual tensile and compressive stresses, respectively. A tensile residual stress will act to extend the stress-free crack so that $C > C_0$, while a compressive residual stress will shorten it so $C < C_0$.

The objective of this paper is to investigate the effect of number of layers, their thickness and thermal properties on the level of residual stress developed in the layers of the laminates. Also, an additional objective of this paper was to study the role of the residual stress in toughening of the laminated composites.

2. Experimental procedure

$\text{Si}_3\text{N}_4/\text{BN}$ based laminates were slip-cast alternately with Si_3N_4 layers and BN based interfaces in plaster of Paris mould in a casting chamber of rectangular/square cross-section of 8 mm \times 8 mm and \sim 60 mm deep. All laminates were fabricated in such a way that the outside layer and core are Si_3N_4 .

Two types of laminated materials were fabricated and studied in this paper. One consists of Si_3N_4 layers and BN based interface with 90 wt.% of BN and 10 wt.% Si_3N_4 marked as SN – (SN + BN). The other one consists of Si_3N_4 layers and BN based interface with 50 wt.% of BN and 50 wt.% of Al_2O_3 marked as SN – (BN + Al_2O_3). For any given number of Si_3N_4 layers, which varied from 3 to 19, 3–5 samples were fabricated and sintered having the size of the samples after sintering of $\sim 6 \text{ mm} \times 6 \text{ mm}$ in cross-section and $\sim 50 \text{ mm}$ in length. In the SN – (SN + BN) class of laminates, the Si_3N_4 layer thickness varied from ~ 70 to $\sim 510 \mu\text{m}$, and in the SN – (BN + Al_2O_3) class of laminates the Si_3N_4 layer thickness varied from ~ 80 to $\sim 320 \mu\text{m}$. After sintering the samples were sliced in the direction parallel to samples' cross-section and the cross-sections of the sliced pieces were polished.

In order to determine crack size and, in turn, residual stress field, Vickers' indentations were made in both bulk, un-layered, structure (produced by the same slip casting method using the same Si_3N_4 -based slurry as in concentric $\text{Si}_3\text{N}_4/\text{BN}$ laminated structures) and in laminated $\text{Si}_3\text{N}_4/\text{BN}$ structures. For the indentation results, five tests were conducted in order to obtain the crack length. The indentation load varied from 5 to 50 kg. The indentations were made within Si_3N_4 layer as well as in a solid un-layered Si_3N_4 core. After indentations, samples were sputtered with gold and the crack lengths of the probing indents were measured by SEM and optical microscopy. During indentation of laminated structures, appropriate care was taken to orient (direct) the indenter in such a way that two corners of the Vickers indentation were directed to the BN-based interface and the other two to the Si_3N_4 layers. After indentations, the cracks were examined and their lengths measured to determine the magnitude of residual stress. In the SN – (SN + BN) class of laminates the measured half size of the crack varied from ~ 102.5 to $202.9 \mu\text{m}$, which depends on used load and the number of Si_3N_4 layers, while in the SN – (SN + BN) class of laminates the measured half size of the crack varied from ~ 153.25 to $\sim 196.75 \mu\text{m}$. For example, the measured half crack size in SN – (SN + BN) laminates with seven layers under the 30 kg load was $153.3 \mu\text{m}$. However, the measured half size of the crack under the same load in SN – (SN + BN) laminates with 7 Si_3N_4 layers was $114.4 \mu\text{m}$. Under the same load the half size of the crack in conventional non-laminated Si_3N_4 was considerably larger $\sim 205 \mu\text{m}$.

3. Results and discussion

In the $\text{Si}_3\text{N}_4/\text{BN}$ laminates the material with lower thermal expansion coefficient is the Si_3N_4 with $\alpha = 3.2 \times 10^{-6}/^\circ\text{C}$. The phase with higher thermal expansion is the interfacial YAG phase² which is formed as a result of reaction between Al_2O_3 and Y_2O_3 and has the thermal expansion coefficient of $\sim 8 \times 10^{-6}/^\circ\text{C}$. Substituting appropriate values for $\nu_{\text{SN}} = 0.22$, $E_{\text{SN}} = 320 \text{ GPa}$, $\alpha_{\text{SN}} = 3.2 \times 10^{-6}/^\circ\text{C}$, the average layer thickness of $t_1 = 230 \times 10^{-6} \text{ m}$, $\nu_{\text{interf.}} = 0.25$, $E_{\text{interf.}} = 390 \text{ GPa}$, $\alpha_{\text{interf.}} = 8 \times 10^{-6}/^\circ\text{C}$, $t_2 = 15 \times 10^{-6} \text{ m}$ and $\Delta T = (1300 - 20)^3$ in Eqs. (2) and (3) gives value for the residual compressive stress in SN – (BN + Al_2O_3) of $\sim 220 \text{ MPa}$

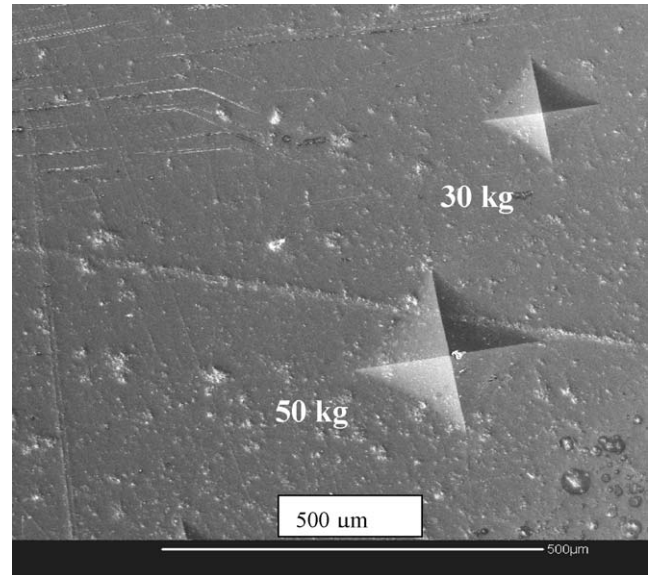


Fig. 2. Vickers indentations made under loads of 30 and 50 kg in Si_3N_4 core with 7 Si_3N_4 layers in SN – (BN + Al_2O_3) laminate.

for laminates with 7 Si_3N_4 layers. The same calculation, using Eqs. (2) and (3), was done for SN – (BN + SN) laminate with 4 Si_3N_4 layers. In this laminates, the calculation was based on the assumption that the interface consists of 90 wt.% BN and 10 wt.% Si_3N_4 . Since the hexagonal BN has high anisotropy in the thermal expansion coefficient in (0001) direction ($\alpha = 3.8 \times 10^{-6}/^\circ\text{C}$) and (1000) direction ($\alpha = -2.7 \times 10^{-6}/^\circ\text{C}$), and considering that the BN interface was polycrystalline phase, the level of anisotropy in thermal expansion will likely be reduced by random orientation of the BN and Si_3N_4 grains in three dimensions.¹⁶ The thermal expansion coefficient of BN phase was estimated to be $\alpha = 10.86 \times 10^{-6}/^\circ\text{C}$. The values for Poisson's ratio, Young's modulus and thermal expansion coefficient of the interface were calculated using the rule of mixture. Substituting values for $\nu_{\text{interf.}} = 0.202$, $E_{\text{interf.}} = \sim 90 \text{ GPa}$, $\alpha_{\text{BN+SN}} = 10.24 \times 10^{-6}/^\circ\text{C}$ and $t_2 = 15 \times 10^{-6} \text{ m}$, with the same values for Si_3N_4 as in SN – (BN + Al_2O_3) laminates but different layer thickness of $t_1 = 445 \times 10^{-6} \text{ m}$ in Eqs. (2) and (3), the calculated residual stress is found to be $\sim 40 \text{ MPa}$.

Fig. 2 shows the indentations in SN – (BN + Al_2O_3) made under the loads of 30 and 50 kg in the Si_3N_4 solid core for a laminate with 7 layers. As it can be seen, no cracks are developed even under the load of 50 kg. Based on this, one can conclude that high residual stress (compressive in nature) was present in the core of the laminate. Due to the fact that no cracks were developed even under the load of 50 kg, a lower bound value for the residual stress was determined by using the length of a diagonal of the indentation rather than the crack length. This clearly shows that strong compressive residual stress exists within the core of the laminate which prevents opening of the cracks.

Based on the crack/diagonal size in the stressed and unstressed Si_3N_4 , the calculated values for compressive residual stress was determined using Eq. (8) and presented in Figs. 3 and 4. It is interesting to note that the maximum stress

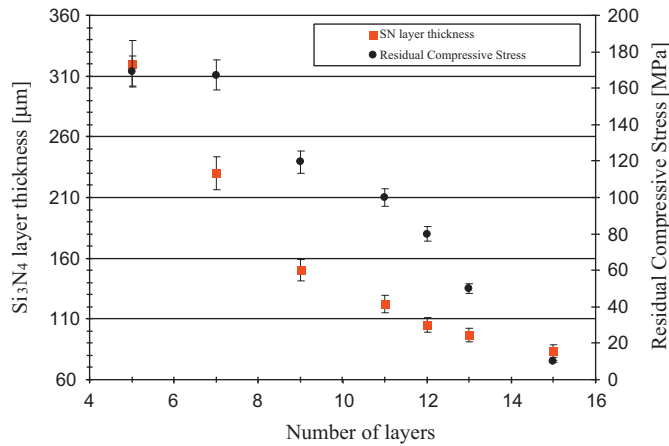


Fig. 3. Residual stress vs. number of Si₃N₄ layers and their thickness in SN – (BN + Al₂O₃) laminates.

occurs at a lower number of layers (3–5) and decays to zero at approximately 15 layers. Also, much higher residual stress was measured in SN – (BN + Al₂O₃) laminates (~170 MPa) than in SN – (BN + SN) laminates (~75 MPa).

Here, it should be indicated that the increase in the number of layers is not the only cause for the decrease in residual stress. Another factor is the layer thickness, which goes down as the number of layers in the laminates goes up. It is believed that the decrease in residual stress is caused by the decrease in the layer thickness, as predicted by Eq. (2). Thin Si₃N₄ layers allow much faster relaxation of residual stress than the thicker ones. In addition to Si₃N₄ layer thickness, porosity in the interfacial layer is another factor which determines the level of residual stress. It is shown by Boccaccini¹⁷ that, increased porosity in one of the composite's (laminate's) constituents, results in a decrease of residual stresses. As discussed in previous publication,^{2,3} an increase in the number of layers increases the level of porosity in both class of laminates and consequently lowers the level of residual stress in the layers. The increased level of porosity corresponds to the porosity level in the samples as the number of "porous" BN-based interfaces increases.² On the other hand, the increased number of layers decreases the Si₃N₄ layer thickness; but then the densities of the Si₃N₄ layers go up. Even though

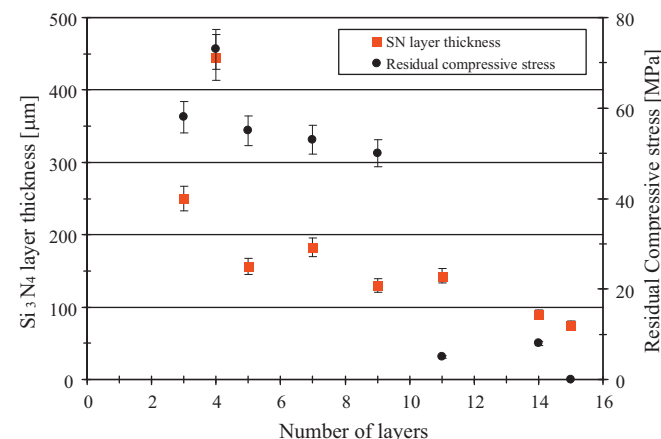


Fig. 4. Residual stress vs. number of Si₃N₄ layers in SN – (BN + SN) laminates.

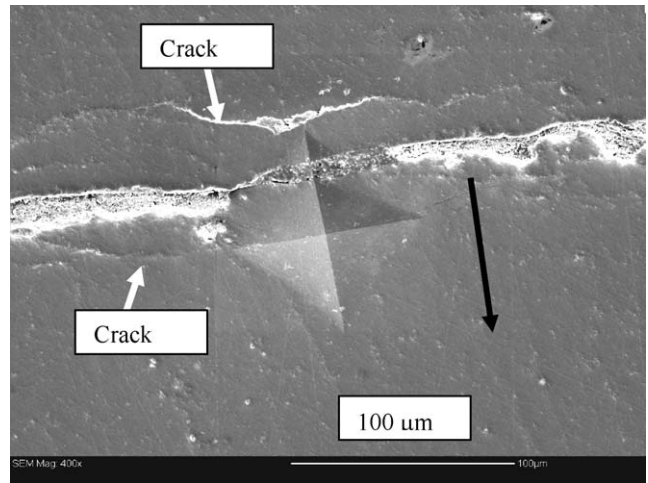


Fig. 5. Vickers indentation made under the load of 20 kg in Si₃N₄ layer of SN – (BN + Al₂O₃) laminates (black arrow points to the center of the sample).

the determination of the level of porosity in the Si₃N₄ layers was relatively difficult, after careful examination of the Si₃N₄ layer's microstructure under SEM, it was found that the level of porosity in the Si₃N₄ layers was very small^{2,3} and estimated to be less than 2% (Figs. 5–9). At this juncture, since the level of porosities in the BN-based interfaces was kept constant during slip-casting of the laminates one may conclude that the layer thickness (accordance with Eq. (2)) is the predominant factor (excluding the diffusion processes during sintering), which controls the level of residual stress or stress relaxation in both class of laminates.

The highest residual stress of ~75 MPa was determined in samples with 4 Si₃N₄ layers, while the lowest one of ~2 MPa in samples with 15 layers. The results shown in Figs. 3 and 4 also indicate that the level of residual stress is strongly affected by the Si₃N₄ layer thickness and this plays very important role in controlling the overall apparent fracture toughness.³ In the SN – (BN + Al₂O₃) class of laminates, the highest residual

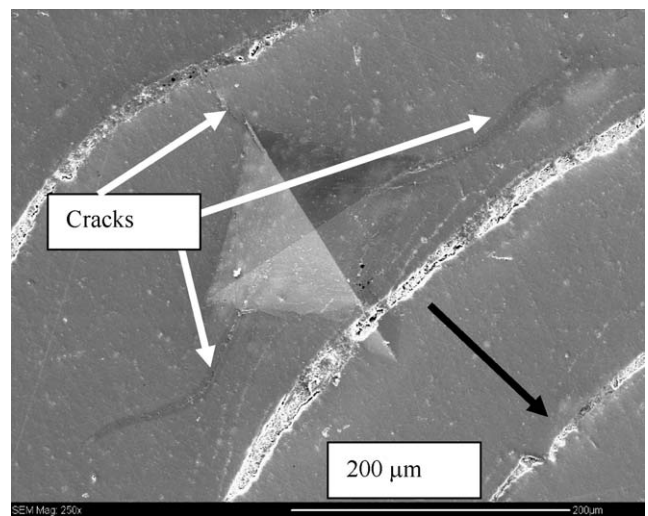


Fig. 6. Vickers indentation under the load of 25 kg in SN – (BN + Al₂O₃) laminated structure with 12 Si₃N₄ layers (black arrow points to the center of the sample).

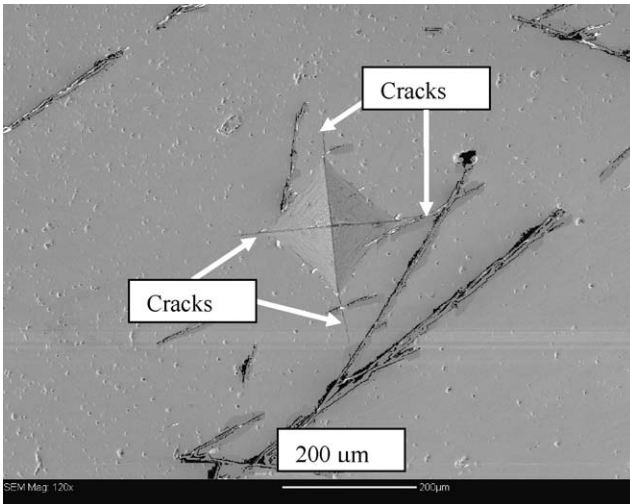


Fig. 7. Vickers indentation under the load of 25 kg in the Si_3N_4 core of SN – (BN + SN) laminated structure.

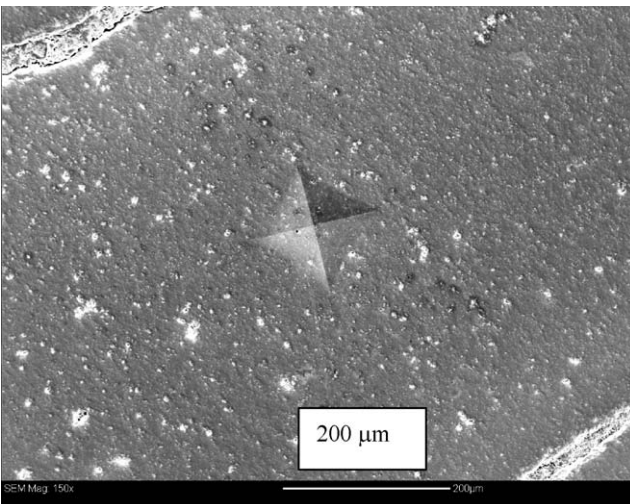


Fig. 8. Vickers indentation under the load of 20 kg in SN – (BN + SN) laminated structure.

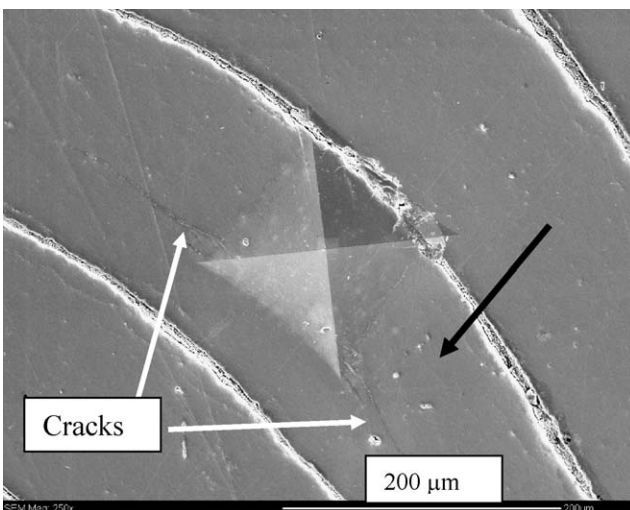


Fig. 9. Vickers indentation under the load of 30 kg in SN – (BN + SN) laminated structure (black arrow points to the center of the sample).

stress was observed in laminates having 5 Si_3N_4 layers with an average layer thickness of $320\ \mu\text{m}$. At the same time, in this class of laminates, the highest apparent fracture toughness of $22\ \text{MPa m}^{1/2}$ was measured in the laminates having 7 Si_3N_4 layers with an average layer thickness of $230\ \mu\text{m}$.³ A different maximum in fracture toughness and residual stress, at the particular Si_3N_4 layer thickness, is believed to be due to different ratios of Si_3N_4 layer thickness to BN-based interlayer thickness. As Fig. 3 shows, the increase in number of layers decreases the level of residual stress. Therefore, an additional possible reason for the reduction of apparent fracture toughness as the number of layers increases³ could be the reduction of the residual thermoelastic stress itself which also changes with the thickness of the layers (Figs. 3 and 4). In the SN – (BN + SN) class of laminates, the maximum apparent fracture toughness of $19.5\ \text{MPa m}^{1/2}$ ³ and residual stress of 75 MPa were observed at the same Si_3N_4 layer thickness of $450\ \mu\text{m}$. In this case, probably this layer thickness provides the best condition for achieving the highest apparent fracture toughness and residual stress. Further increase in the number of Si_3N_4 layers decreases both toughness and the residual stress. This indicates that the Si_3N_4 layer thickness controls the both. At this point, the same conclusion can be made that as the number of layers increases the layer's thickness decreases, leading to the relaxation of residual stress (Eq. (2)). Since the level of residual stress controls the apparent fracture toughness, one may conclude that the major reason for the decrease in the apparent fracture toughness in this laminates is in fact decrease of residual stress itself.

In order to verify the presence of residual stresses in both laminates, Vickers indentation was made in SN – (BN + Al_2O_3) laminates with 7 Si_3N_4 layers (Fig. 5). No cracks are observed in any of the four corners of the indentation confirming the presence of compressive stress in the Si_3N_4 layers acting against opening of the crack. The load of 20 kg is normally sufficient to create a large crack in a monolithic stress-free Si_3N_4 . The first cracks appeared at loads $>25\ \text{kg}$ and only in the direction parallel to the interface (Fig. 6).

Based on the crack length, applied load and Young's modulus, the fracture toughness was calculated to be between 12 and $15\ \text{MPa m}^{1/2}$, depending on the crack size. Considering that the fracture toughness of a monolithic Si_3N_4 is between 8.5 and $9.6\ \text{MPa m}^{1/2}$ (calculated by Eq. (5)), the fracture toughness of a single Si_3N_4 layer is considered to be very high. One possible reason for the much higher fracture toughness of the laminates is the presence of compressive stress parallel to the direction of the interface.

Quite different behaviour was observed in SN – (BN + SN) laminates. Unlike SN – (BN + Al_2O_3) laminates, cracks were observed at all four corners of the Vickers indentation (Fig. 7). Although the indentation cracks were much shorter than in the monolithic/unstressed Si_3N_4 materials, the fracture toughness in these laminates was estimated to be $\sim 13\ \text{MPa m}^{1/2}$, which is considerable above that of monolithic Si_3N_4 ceramics. This serves as a proof that, although the residual stress does exist in the layers, its magnitude is smaller than that in the SN – (BN + Al_2O_3) laminates.

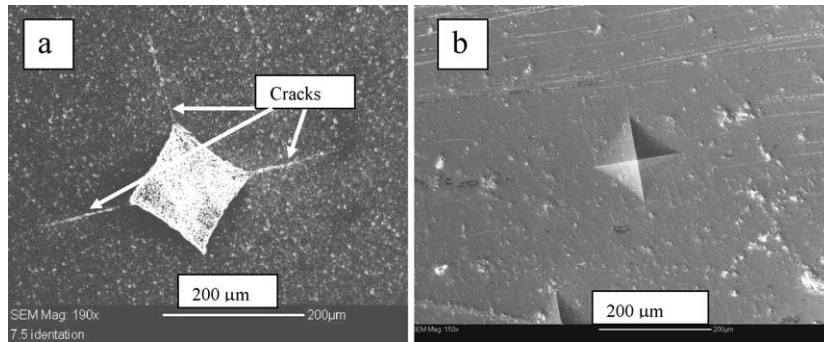


Fig. 10. Comparison of crack lengths developed under the same load of 30 kg in (a) unstressed monolithic Si_3N_4 ($K_{IC} = 7.98 \text{ MPa m}^{1/2}$) and (b) stressed $\text{Si}_3\text{N}_4/\text{BN}$ -based laminated structures ($K_{IC} = 18.87 \text{ MPa m}^{1/2}$).

In order to systematically analyze the effect of residual stress on crack initiation, and direction of crack propagation, additional indentations were made in Si_3N_4 layers in samples with different number of layers. The rationale for making indentations at different places with different indentation's orientation, lies in the intention to investigate nature or direction of crack propagation in the presence of residual stress located at different sites in the laminates. In the cases where cracks did not appear (e.g. within the Si_3N_4 layers) served as an indication of the presence of strong residual stress, compressive in nature.

Fig. 8 shows the indentation in a single Si_3N_4 layer created under the load of 20 kg. Again, although cracks were observed at the corners of the indentation, their length was relatively small. When the indentation load was increased to 30 kg (Fig. 9), large cracks were observed but again, only in the direction parallel to the interface.

In order to further appreciate the level of toughening and the consequent increased resistance to crack propagation in the presence of residual stress, Fig. 10 shows the indentations made in monolithic Si_3N_4 and in laminated Si_3N_4 ceramics. While cracks larger than $300 \mu\text{m}$ were observed in unstressed monolithic Si_3N_4 no cracks were detected in $\text{SN} - (\text{BN} + \text{Al}_2\text{O}_3)$ laminates. During sintering of the laminates, the Y_2O_3 sintering aid employed to enhance densification in Si_3N_4 layers also diffuses through the interface and reacts with Al_2O_3 to form the eutectic glassy phase which increases the bonding between the layers.²

In layers where Al_2O_3 is absent, such as is the case in $\text{SN} - (\text{BN} + \text{SN})$ laminated structure, the amount of glassy phase is too small to be able to create a strong interface. When 50 wt.% of Al_2O_3 is added to the BN interface the two phases present in the interface are Al_2O_3 and YAG ceramics.² Since there is a large difference between the thermal expansion coefficients of Al_2O_3 ($8.9 \times 10^{-6}/^\circ\text{C}$), YAG ($\sim 8 \times 10^{-6}/^\circ\text{C}$) and Si_3N_4 ($\sim 3.2 \times 10^{-6}/^\circ\text{C}$) (20–1000 °C) the interface will shrink more than the Si_3N_4 layers on cooling from the fabrication temperature and will be subjected to tensile stress while Si_3N_4 layers will be under compressive stress. This effect is especially strong when bonds between Si_3N_4 layers and the interface are stronger such as is the case with $\text{SN} - (\text{BN} + \text{Al}_2\text{O}_3)$ laminated structure.

The interfacial stress developed as a result of difference in thermal expansion between Si_3N_4 layers and BN interface was found to be an important factor which controls the crack ini-

tiation and its propagations in laminates studied in this paper. Also, it is believed that this new laminated structures offers great potential in developing reliable high toughness ceramics in a cost effective manner. Further optimization of the layers thickness, their chemistry and microstructure may lead to yet further improvement of mechanical properties and we are still far from reaching full potential of the structure.

4. Conclusion

The level of residual stress developed in the interface was found to depend on the nature/composition of the interface and Si_3N_4 layer thickness. The compressive stress of 170 MPa, was found to exist in higher density inter-layers of $\text{SN} - (\text{BN} + \text{Al}_2\text{O}_3)$ laminates compared to the stress of 75 MPa in lower density inter-layers of $\text{SN} - (\text{BN} + \text{SN})$ laminates. Both, the residual stress and the interfacial strength govern the direction of crack propagation which, in turn, controls the fracture resistance of the $\text{Si}_3\text{N}_4/\text{BN}$ laminates.

This residual compressive stress is one of the main reasons why $\text{SN} - (\text{BN} + \text{Al}_2\text{O}_3)$ laminates exhibit significantly high apparent fracture toughness³ compared to $\text{SN} - (\text{BN} + \text{SN})$.

Unlike $\text{SN} - (\text{BN} + \text{Al}_2\text{O}_3)$ laminates, which contain a much lower level of porosity and considerable amount of glassy phase,² $\text{SN} - (\text{BN} + \text{SN})$ laminates have lower density (higher porosity) and no YAG or glassy phase in the interface. This makes the interface much weaker allowing the crack to deflect and travel longer distances before it is arrested and forced to change its direction of propagation. The consequence of this is the relaxation of residual stress in the Si_3N_4 layers. The absence of a strong interfacial layer makes it easier for the crack to be reinitiated and propagated at the next Si_3N_4 layer.

References

1. Yu Z, Krstic Z, Krstic VD. Laminated $\text{Si}_3\text{N}_4/\text{SiC}$ composites with self-sealed structure. *Key Eng Mater* 2005;**280–283**:1873–6.
2. Krstic Z, Krstic VD. Young's Modulus, density and phase composition of pressureless sintered self-sealed $\text{Si}_3\text{N}_4/\text{BN}$ laminated structures. *J Eur Ceram Soc* 2008;**28**:1723–30.
3. Krstic Z, Krstic VD. Fracture toughness of concentric Si_3N_4 -based laminated structures. *J Eur Ceram Soc* 2009;**29**:1825–9.
4. He MY, Hutchinson JW. Crack deflection at the interface between dissimilar elastic materials. *Int Solids Struct* 1989;**25**(9):1053–67.

5. He MY, Heredia FE, Wissuchek DJ, Shaw MC, Evans AG. The mechanics of crack growth in layered materials. *Acta Met Mater* 1993;**41**(4):1223–8.
6. Hsueh CH, Evans AG. Residual stresses and cracking in metal/ceramic system for microelectronics packaging. *J Am Ceram Soc* 1985;**68**(3):120–7.
7. Evans AG, Lu MC, Schmauder S, Ruhle M. Some aspects of the mechanical strength of ceramic/metal bonded system. *Acta Metall* 1986;**34**(8):1643–55.
8. Chen Z, Mecholsky JJ. Toughening by metallic lamina in nickel/alumina composites. *J Am Ceram Soc* 1993;**76**(5):1258–64.
9. Yttergren R-MF, Zeng K, Rowcliffe DJ. Residual stress and crack propagation in laminated composites. *Advances in ceramic–matrix composites II, ceramic transactions*, vol. 46. The American Ceramic Society; 1995. p. 543–53.
10. Oechsner M, Hillman C, Lange FF, Suo Z. Surface cracking in layers under biaxial, residual compressive stress. *J Am Ceram Soc* 1995;**78**(9):2353–9.
11. Blugan G, Dovedoe R, Gee I, Orlovskaya N, Kuebler J. Failure behaviour of high toughness multi-layer Si_3N_4 and Si_3N_4 –TiN based laminates. *Fractogr Adv Ceram II* 2005:175–82.
12. Marshall DB, Lawn BR. An indentation technique for measuring stresses in tempered glass surfaces. *J Am Ceram Soc* 1977;**60**(1–2):86–7.
13. Zeng K, Rowcliffe D. Experimental measurement of residual stress field around a sharp indentation in glass. *J Am Ceram Soc* 1994;**77**(2):524–30.
14. Evans AG, Charles EA. Fracture toughness determination by indentation. *J Am Ceram Soc* 1976;**59**(7–8):371–2.
15. Lawn BR. Fracture of brittle solids. In: *Cambridge solid state science series*. 2nd ed. Cambridge, UK: Cambridge University Press; 1993. p. 31.
16. Schapery RA. *J Compos Mater* 1969;**2**:311.
17. Boccaccini AR. Incorporation of porosity to control the residual thermal stresses in ceramic composites and laminates. *Eur Phys J AP* 1998;**2**:197–202.